

# Air Solar Collectors with Baffles: Aerodynamics, Heat Transfer and Efficiency

**Ben Slama R.\* , Bouabdallah M.\*, and Mora J.C\*\***

\* Laboratoire de Génie des Procédés. Ecole Nationale d'Ingénieurs de Gabès.  
Route de Médenine, 6029, Gabes, TUNISIA

\*\* Institut National Polytechnique de Toulouse-ENSIGC  
31078 Toulouse, FRANCE

## ABSTRACT

*The paper presents the study on different air collectors with different-flow patterns. The use of baffles creates the turbulence of the hot air carrier and thus increases the collector's efficiency. The diverse types of air collectors are principally those for which air passes above or below the absorber, or at first above then below. The contribution of this study in the field of air solar collectors consists of measurement of heat losses and the estimation of efficiency of two types of collectors based on assumed flows. Smaller baffles create weak turbulence. The gain in efficiency compared to collectors without baffles is about 25 %. The bigger transversal baffle occupies 72 % of the collector's width. Combined with smaller baffles, placed longitudinally, this gives a meandering flow and promotes turbulence. Thus the efficiency is increased by approximately 60 % compared to collectors without baffles.*

## NOMENCLATURES

$A$	Surface area of collector	$m^2$	surface area)	$kg/sm^2$
$b$	Air channel thickness	$m$	$Nu$	Nusselt number
$cp$	Specific heat	$J/kgK$	$Qv$	Air flow rate (volume) per unit of surface area
$D$	Hydraulic diameter	$m$		$m^3/sm^2$
$d$	Thickness of still air layer	$m$	$Re$	Reynolds number
$eb$	Thickness of insulator	$m$	$S$	Air flow section
$g$	Acceleration due to gravity	$m/s^2$	$T$	Temperature
$Gr$	Grashof number		$U_b$	Overall losses coefficient (back of collector)
$h_{xy}$	Heat transfer coefficient between surfaces "x" and "y"	$W/mK$	$V$	Air velocity
$h_{cxy}$	convective heat transfer coefficient	$W/m^2K$	$\alpha$	Solar absorptance of the absorber plate
$h_{rxy}$	Radiative heat transfer coefficient between surface "x" and "y"	$W/m^2K$	$\beta$	Coefficient of thermal expansion of air
$i$	Delta wing incidence	$d^\circ$		$1/d^\circ$
$I_N$	Incident solar flux	$W/m^2$		or Wing opening angle
$L$	Length of collector	$m$	$\gamma$	Angle between whirls and delta wing
$l$	Width of collector	$m$		$d^\circ$
$m$	Air flow rate (mass per unit of		$\mu$	Air dynamic viscosity
				$kg/ms$

$\rho$	Density	kg/m <sup>3</sup>	$A$	Surrounding air
$\lambda$	Thermal conductivity	W/mK	$b$	Insulator
$\sigma$	Stephens constant	W/m <sup>2</sup> k <sup>4</sup>	$c$	Sky
$\varepsilon$	Emissivity coefficient		$p$	Absorber
			$s$	Exit
			$v$	Glass or wind
			$T$	Temperature

### Symbols

$a$  Air flowing inside the solar collector

## 1. INTRODUCTION

The present development of solar collectors, essential elements to any solar equipment, is due to a world consciousness of the importance of solar energy. The characteristics of simplicity, reliability and efficiency of these collectors are not always simultaneously ensured, and are often much debated. Air collectors have a low thermic inertia because the specific heat of air is as low as that of water. Little air leaks do not alter, in large proportion, the efficiency of air collectors. Conversely, the air collector efficiency is lower than that of water collectors because of low thermal exchange between air and the absorber, and the structure of air collectors is lighter than that of water collectors. The aim of this article is to show how to improve heat transfer efficiency (Figs. 1 - 2) by using appropriate baffles. The hot air obtained can be used to heat buildings and dry fruit, vegetables and meat.

## 2. PARAMETERS INFLUENCING THE INSTANTANEOUS EFFICIENCY OF AIR COLLECTORS

The efficiency equation of an air collector is :

$$\eta = Q_{VT} \rho_T C p_a \Delta T / I_N \quad (1)$$

The different types of air collectors were compared considering uniform measuring conditions and the same air flow rate. The best collector develops the highest temperature increase  $\Delta T$  of caloporting air, and thus have the highest efficiency. To improve  $\Delta T$ , it is important to reduce the collector's thermal losses and particularly to improve the heat transfer between the absorber and caloporting air.

The reduction of thermal losses when the temperature is high is achieved through a good choice of the material and thickness of the insulator, and of the glass.

To improve the transfer, different configurations have been proposed :

- Small fins under the absorber in order to increase the exchange area [1,2], and
- Selection of flow patterns [3,7] (Fig.3). Only few experiments have been documented that used obstacles in air flow channels in order to promote turbulence [8-12]. Biondi [6], in order to compare different collectors, has introduced a geometrical coefficient,  $K$ , using the collector's length,  $L$ ; the air flow channel thickness,  $b$ ; and the hydraulic diameter,  $D$ , as:

$$K = \frac{L}{b D^{0.25}} \quad (2)$$

The importance of the quantity  $K$  is fundamental since it is easy to prove that the coefficient of the convective exchange, for the same values of  $m$  and  $K$ , is a constant, unless there are variations



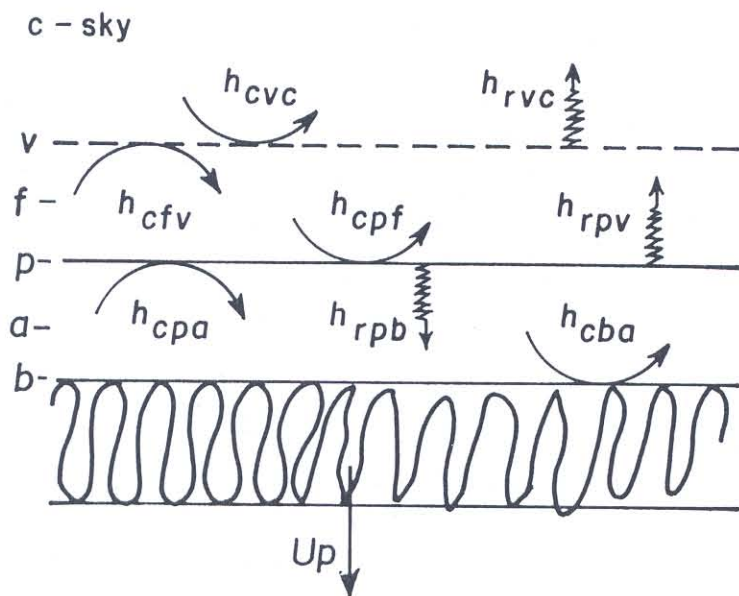


Fig. 1. Heat transfer process: non steady state.

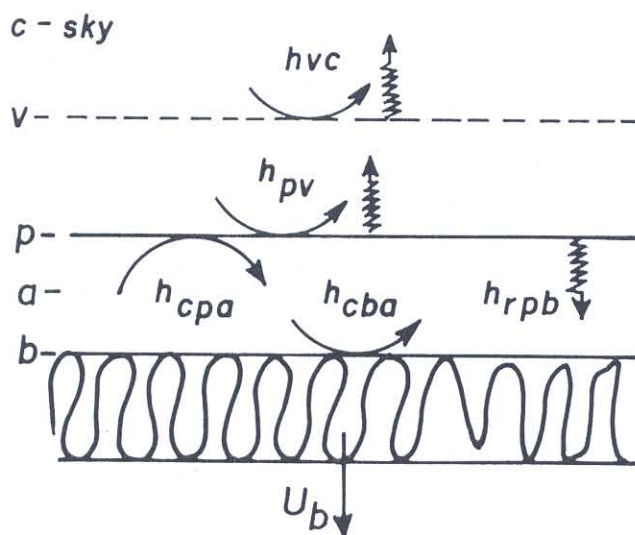


Fig. 2. Heat transfer: steady state.

of second order with temperature. Considering:

As per the definition of the mass flow :  $m = VS \rho/A = Vb \rho/L$  (3)

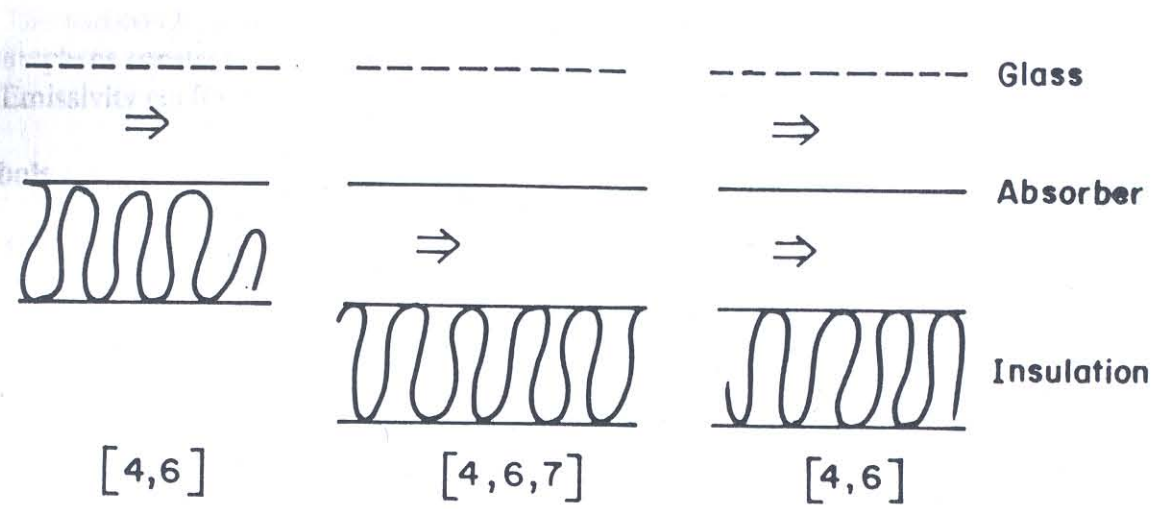
The air velocity is :  $v = mL / b\rho$  (4)

Introducing  $K$  :  $v = mKD^{0.25} / \rho$  (5)

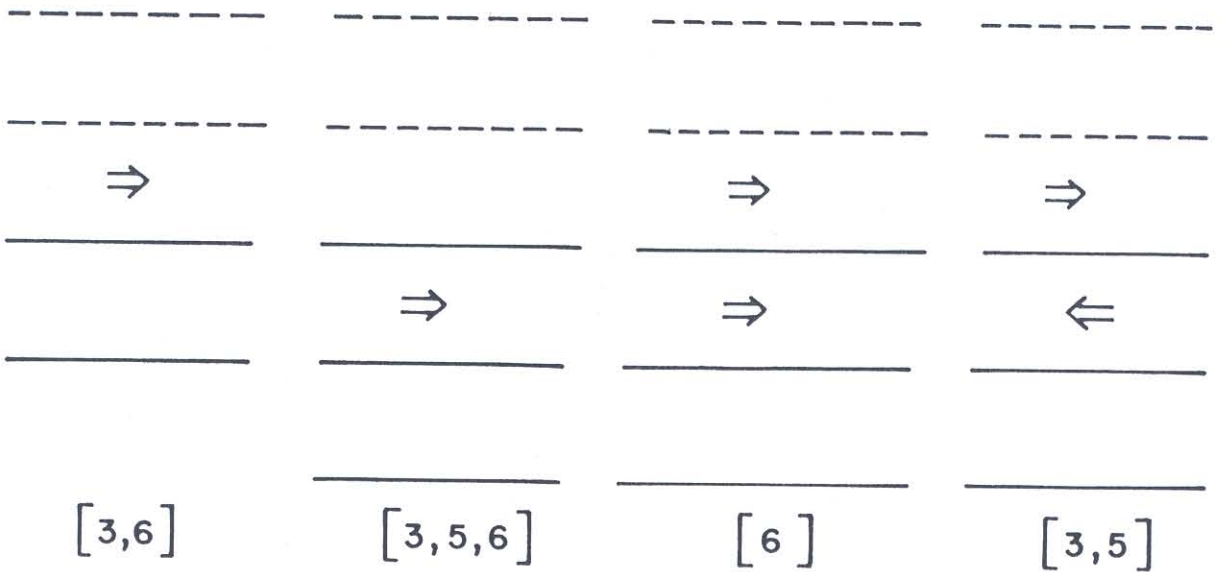
The Reynolds' number is:  $Re = VD \rho/\mu = (mKD^{1.25})/\mu$  (6)

Assuming that the exchange by convection is determined by Kay's relation (turbulent flow between two parallel plates), Nusselt's number is :

$$Nu = 0.0158 Re^{0.8} \text{ or}$$



with simple glass



with double glass

Type 1-a

Type 1-b

Type 1-c

Type 1-d

Fig. 3. Different types of air flows in solar collectors.

Type 1-a: Air flow above absorber; Type 1-b: Air flow below the absorber;  
Type 1-c: Air flow above and below the absorber; Type 1-d: Air flow above then below the absorber.

$$Nu = 0.0158 (mK/\mu)^{0.8} D \tag{7}$$

Finally the heat transfer coefficient is :

$$hc = Nu \lambda/D$$

$$hc = 0.0158 (mK/\mu)^{0.8} \tag{8}$$

The results obtained by Biondi shows that for high values of  $K$ , the collector with two air flow channels type 1-b has an efficiency better than the collector type 1-c with two parallel flows, particularly for  $\Delta T/I_N$ . Wijesundera [5] uses a collector type 1-d and compares it to collector type 1-b. For a high ratio  $\Delta T/I_N$  (0.05 to 0.06  $m^2\text{°C}/W$ ), the efficiency of type 1-b collector is close to that of type 1-d. Type 1-b with baffles would exceed the results of 1-d as shown by the measurements to show the advantages of a collector with baffles vis à vis collectors without baffles [9].

- Finally Choudhury and Garg [7] study a collector with air jet with the air flow rate of the device ranging from 50  $m^3/h/m^2$  to 250  $m^3/h/m^2$ . This is compared to the collectors with two air channels type 1-b, without baffles. The jet air collector proved better than the type 1-b collectors. The authors tested a type 1-b collector with a thickness "b" being 0.1 m and 0.05 m. The result confirms that the efficiency increases as the thickness diminishes. Using baffles in the mobile air vein with a view to promoting heat transfer, would have reached better efficiencies for air delivery, clearly lower than 50  $m^3/h/m^2$  [8-11].

### 3. TWO AIR CHANNEL TYPE 1-b COLLECTORS WITH BAFFLES

The collectors used two air channels type 1-b, one for flowing air and the other for still air (Fig. 4). It is the only efficient way to use baffles to promote turbulence, hence, the heat transfer coefficient and consequently the collector's efficiency.

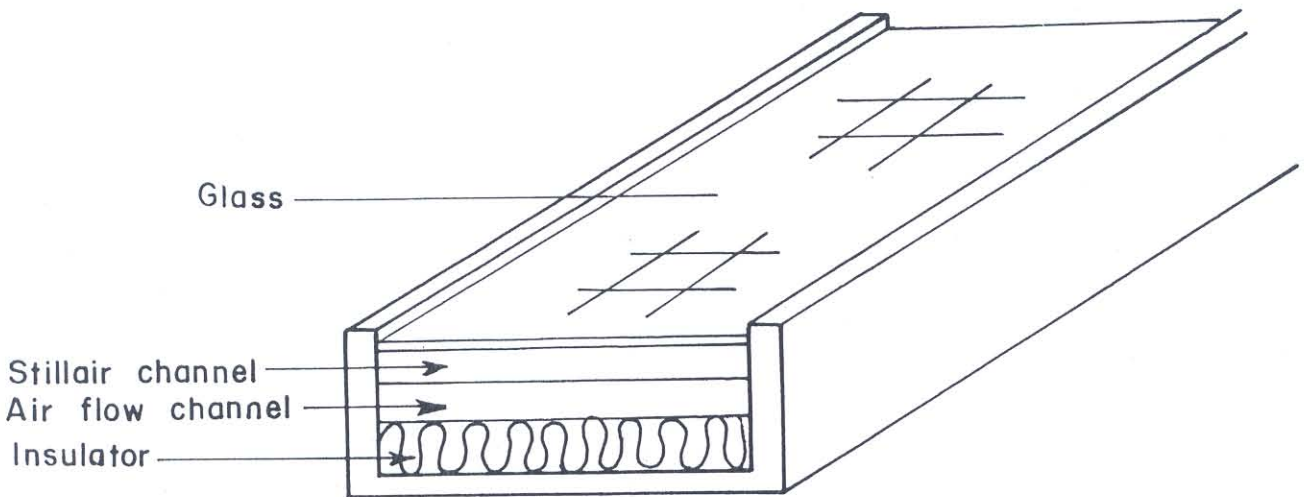
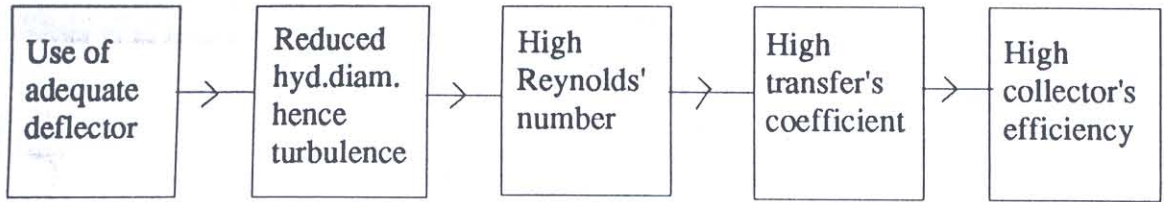


Fig. 4. Air collector with air channels type 1-b.



The methodology is as follows:



In order to reduce the equivalent hydraulic diameter, the thickness "b" has been reduced and the "l" width of the passage of caloporting air in the collector was created, with appropriate baffles causing a winding flow, hence doubling the length of the trajectory of caloporting air in the collector (Fig.5). This concurred with Biondi [6], concerning the geometrical coefficient K.

The effect of the baffle is the creation of turbulence, in such a way as to make the air, licked the hot surface of the absorber and to decrease the thermal sublayer. For these reasons, the baffles are placed on the insulation. The space between the absorber and the glass reduces the convective losses at the front side.

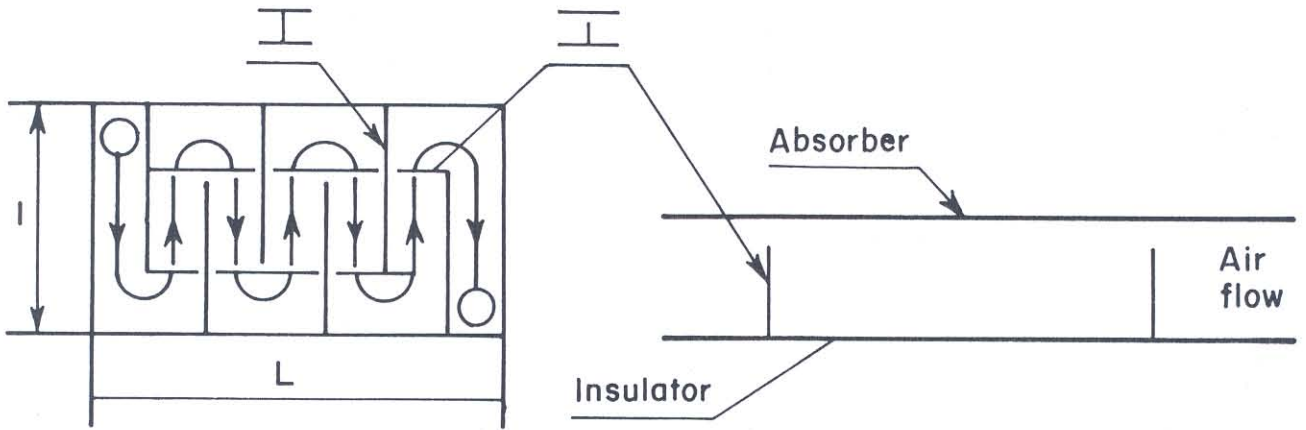


Fig. 5. Meandering flow with mixed baffles type 14 - 6: whirls formation.

#### 4. MODELS OF COLLECTOR TYPE 1-b

##### 4.1 Energy Balance: Transient Regime

According to Bhargava-Garg and Sharma [4] the equation for the different components are as follows (Fig. 2):

*Glass*

$$M_v c p_v \frac{\partial T_v}{\partial t} = \alpha_v I_N + h_{rpv} (T_p - T_v) + h_{cfv} (T_f - T_v) - h_{cvA} (T_v - T_A) - h_{rvc} (T_v - T_d) \quad (9)$$

**Air between the glass and the absorber (still air)**

$$M_{fcp_a} \frac{\delta T_f}{\delta t} = h_{cpf} (T_p - T_f) - h_{cfv} (T_f - T_v) \quad (10)$$

**Absorber**

$$M_{p'cp_p} \frac{\delta T_p}{\delta t} = \alpha_p \tau I_N - \lambda_p \frac{\delta^2 T_p}{\delta x^2} - h_{rpv} (T_p - T_v) - h_{cpf} (T_p - T_f) - h_{rpb} (T_p - T_b) - h_{cpa} (T_p - T_a) \quad (11)$$

**Air flow**

$$M_{acp_a} \frac{\delta T_a}{\delta t} = - \frac{mcp_a}{1} \frac{\delta T_a}{\delta x} + h_{cpa} (T_p - T_a) + h_{cba} (T_b - T_a) \quad (12)$$

**Back plate**

$$M_{b'cp_b} \frac{\delta T_b}{\delta t} = -\lambda_b \frac{\delta T_b^2}{\delta x^2} + h_{rpb} (T_p - T_b) - h_{cba} (T_b - T_a) - U_b (T_b - T_A) \quad (13)$$

## 4.2 Energy Balance: Steady State

According to Choudhury and Garg [7] the heat energy balance of each component of the collector is:

**Glass** 
$$h_{vc} (T_v - T_A) = h_{pv} (T_p - T_v) \quad (14)$$

**Absorber** 
$$I_N \tau \alpha = h_{pv} (T_p - T_v) + h_{cpa} (T_p - T_a) + h_{rpb} (T_p - T_b) \quad (15)$$

**Back plate** 
$$h_{rpb} (T_p - T_b) = h_{cba} (T_b - T_a) + U_b (T_b - T_A) \quad (16)$$

**Air flow** 
$$m_a cp_a (T_s - T_A) = h_{cpa} (T_p - T_a) + h_{cba} (T_b - T_a) \quad (17)$$

with  $T_a = (T_A + T_s) / 2$

Substituting  $T_a$  in the three equations and eliminating  $T_p$ ,  $T_v$  and  $T_b$ ; the expression for the outlet air temperature  $T_s$  can be written as :

$$T_s = \frac{(U_5 U_{11} + U_8 U_9) I_N \tau \alpha_a + (U_8 U_{10} + U_7 U_{11}) T_A}{U_6 U_{11} - U_8 U_{12}} \quad (18)$$

The  $U$ 's are defined in the appendix.

Using  $T_s$ , the collector's efficiency is written in a classical way as:

$$\eta = \frac{m_a c p_a (T_s - T_A)}{I_N} \quad (19)$$

The various heat transfer coefficients are as follows:

$h_{vc}$ : glass - atmosphere (sky)

$$h_{vc} = h_v + h_{rvc} \quad \text{with} \quad h_v = 5.7 + 3.8 V_v \quad (20)$$

and

$$h_{rvc} = \frac{\epsilon_v \sigma (T_v^4 - T_c^4)}{T_v - T_A} \quad \text{with} \quad T_c = 0.0552 T_A^{1.5} \quad (21)$$

$h_{pv}$ : absorber - glass

$$h_{pv} = h_{cpv} + h_{rpv} \quad (22)$$

where

$$\begin{aligned} h_{cpv} &= Nu_v \lambda a / d \\ Nu_v &= 0.093 (Gr_v)^{0.31} \\ Gr_v &= g \beta (T_p - T_v) d^3 / \gamma^2 \\ h_{rpv} &= \frac{(T_p^2 + T_v^2) (T_p + T_v)}{1/\epsilon_p + 1/\epsilon_v - 1} \end{aligned}$$

$h_{cpa}$  and  $h_{cba}$ : absorber and insulator - air flow

$$h_{cpa} = h_{cba} = Nu_{pa} \lambda_a / D \quad \text{where} \quad Nu_{pa} = 0.0293 (Re_{pa})^{0.8} \quad (23)$$

$$Re_{pa} = mLD / (b\mu)$$



$h_{rpb}$ : radiation between absorber and insulator

$$h_{rpb} = \frac{\sigma (T_p^2 + T_b^2) (T_p + T_b)}{1/\varepsilon_p + 1/\varepsilon_b - 1} \quad (24)$$

$U_b$ : coefficient of rear losses

$$U_b = \lambda_b / e_b \quad (25)$$

## 5. EXPERIMENTAL STUDY OF THE TWO AIR LAYER COLLECTOR TYPE 1-b WITH OR WITHOUT BAFFLES

The following experimental study is about two air channel collectors type 1-b in which different collectors using different types of baffle are compared to a collector without baffles [9].

Three steps were followed:

- visualization of the air flow according to the baffle type,
- measurement of heat losses related to air flow rate,
- measurement of instantaneous efficiency.

Three types of baffles were tested (Fig. 6):

- small baffles type 14-1 to 3: located in ratter (V-shaped), or in such a way as to form a discontinued transversal line, bent in the direction of the flow or opposite to it, with or without contact to the absorber.
- large baffles type 14-4 and 5: transversally located, with a relative length of 70 % of the collector's width, with or without contact to the absorber. Meandering effects are produced.
- large and small baffles type 14-6: Transversal large baffle in close contact with the absorber and small baffles without contact. The large baffles lengthen the trajectory; conversely the small baffles increasing the chocking of air flow (Fig.5).

### 5.1 Visualization of the air flow

The aim of the study was:

- to show air flow trajectory (straight flow, meander, or both),
- to quantify the surface area of dead flow zones.

White smoke was injected between two parallel plates, the baffles being placed on the lower plate. The upper plate is transparent to allow perpendicular view to these plates.

Symbols used were:

⌊ Baffles placed on the insulator and in close contact with the absorber,

⌋ Baffles placed on the insulator without contact with the absorber,

60 % : Example of baffles' relative length,

23/28: Example of baffles' relative height (case without contact with the absorber).

Fig. 6 gives some information concerning the results rate, and the dead flow zones in each collector.

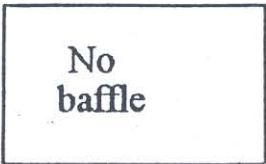
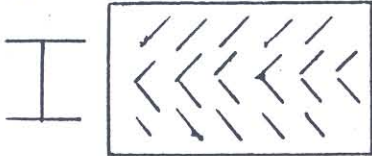
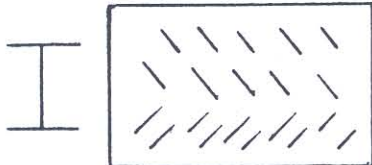
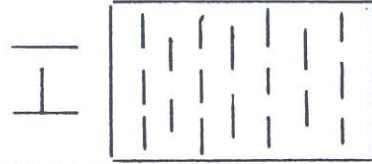
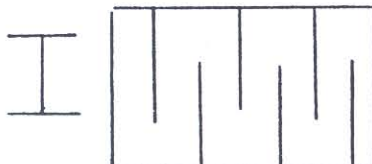
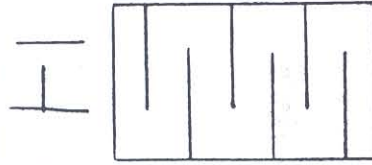
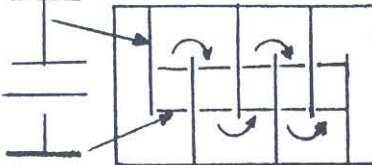
Baffle type	Rate of dead zones		Remarks	An flow length
	20 m <sup>3</sup> /h/m <sup>2</sup>	50 m <sup>3</sup> /h/m <sup>2</sup>		
type 14-0 	25 %	55 %	Direct passage of air in middle of collector with dead zones.	L
type 14-1 	20 %	40 %	Dead zones following the baffles.	L
type 14-2 	15 %	20 %	No stagnation zone.	L
type 14-3 	3 %	4 %	Dead zones only at the exit.	1,1 L
type 14-4 	40 %	50 %	Important dead flow zones following the baffles.	2 L
type 14-5 	10 %	15 %	Interaction of cross-flowing stream following the baffle.	2 L
type 14-6 	3 %	3 %	Whirls.	2 L

Fig. 6. Main visual results.



For collectors type 14-1, 2 and 5, the dead flow zone rate is important and increases with the flow (it is also the case for collectors without baffles). On the other hand, for those type 14-3 and 6 without contact with the absorber, the rate of dead zones remains very low (< 5%).

For type 14-1 to 3, the length of the air flow trajectory is equal to the length of the collector and the passage width is that of the collector. Conversely, for type 14-4 to 6, the trajectory has a length more than double that of the collector and a passage width reduced at less than third of the collector's (two reasons for increasing the air velocity and thus the efficiency).

### 5.2 Pressure Drop Measurement

Turbulence promoters will increase more or less the pressure drop, according to the type of baffles and increase of the electric consumption of the fan (50 W/m<sup>2</sup> of collector for an air flow rate 50 m<sup>3</sup>/h/m<sup>2</sup>).

The losses vary as follows:

- Increases with the air flowrate,
- Decreases as the channel thickness increases,
- Slightly depends on the baffle type,
- Are higher when the baffles, for a same type, are in contact with the absorber,
- Are higher for the large baffles of type 14-4 and 6.

The curves on the Fig. 7 give the pressure drop in mm of water versus the air flow rate. The procedure consists of varying the air flow and measuring with an accurate manometer the pressure drop (difference of pressure per mm of water) between the entry and outlet of the collector, for different types of baffles.

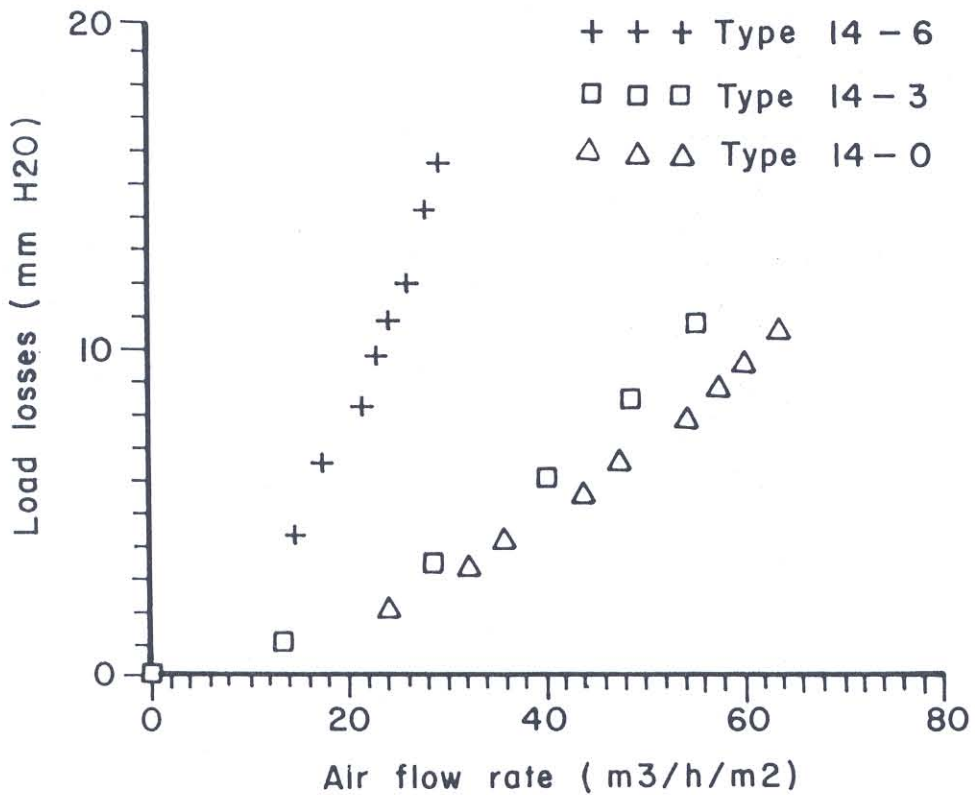


Fig. 7. Load losses in function of air flow rate.



### 5.3 Measurement of Instantaneous Thermal Efficiency

A set of equipment comprising of four identical collectors that can be modified to convert one configuration to another was designed and manufactured (Fig. 4).

The absorber, is made up from a steel sheet, the thickness is one millimeter thick, and painted black. The glass is of double polycarbonate, 8 mm thick. Insulator is made of a 50 mm thick polystyrene sheet protected against heat by a smooth aluminium sheet of 0.05 mm thick, and against weather extremes by a thin wooden plate. The thickness of air channels was 28mm. The wooden case, is recovered with a marine varnish coat to protect it against rain.

The following parameters were measured:

- the temperatures, entry and outlet, of the collector with Iron-Constantan thermocouples.
- the incident flux with a pyranometer or a solarimeter,
- the air velocity with hot wire anemometer or a spinner in a conduit, outlet of the collector, the temperature in the collector to get the density of air for the calculation of efficiency.

Figs. 8 and 9 give, for some types of significant baffles, the efficiency respectively versus the air flowrate and the  $\Delta T / I_N$ .

### 5.4 Discussion

For the same air flow ( $35 \text{ m}^3/\text{m}^2\text{h}$ ), chosen as reference, the collector without baffles showed an efficiency of 38 %, conversely the collector with mixed baffles type 14-6 reaches a 68 % efficiency, which is very high. These results are well in agreement with the models which expects better performances for a collector with a long air path and a low hydraulic diameter (the geometrical coefficient  $K$  introduced by Biondi [6] is then raised).

Thus for a  $900 \text{ W}/\text{m}^2$  incident flux and a useful area of  $100 \text{ m}^2$ :

- the collector without baffles would give only 34,200 Watts, while
- the collector baffle type 14-6 would give 61,200 Watts

Taking an incident solar flux of  $1000 \text{ W}/\text{m}^2$  the abscissa of the curves of Fig. 9 becomes simply  $T_s - T_a$ , the increase in temperature  $\Delta T$ . Then for a 50 % efficiency, the temperature increase could reach  $75^\circ\text{C}$  for a collector with mixed baffles (type 14-6),  $47^\circ\text{C}$  for a collector with small baffles (type 14-3), and only  $21^\circ\text{C}$  for the collector without baffles.

The medium temperature heater ( $90^\circ\text{C}$  to  $110^\circ\text{C}$ ) is thus possible by using mixed baffles, if the entry temperature of the collector is between  $20^\circ\text{C}$  and  $40^\circ\text{C}$  and/or for an incident solar flux ranging from  $700 \text{ W}/\text{m}^2$  to  $1000 \text{ W}/\text{m}^2$ . Actually these climatic conditions are found in hot countries, such as Tunisia, around midday for 4 to 5 hours.

For an incident flux of  $700 \text{ W}/\text{m}^2$  and a 20 W electric consumption for a fan, the latter represents 6.2 % of the useful power produced by a collector without baffles, and only 3.5 % of that produced with baffles type 14-6.

### 5.5 Delta Wing-Shaped Baffles

The other type of baffle is the delta-shaped baffles on which aerodynamics studies have been done [13-15]. The results of the tests showed that an inclined delta wings following " $i$ " incidence is subject to a depression at the extrados (Fig. 10), where whirls formed between them at an angle  $\alpha$  as shown by Fig. 11.

According to  $i$  and  $\alpha$  (wing opening angle), angle  $\alpha$  between whirls takes different values thus

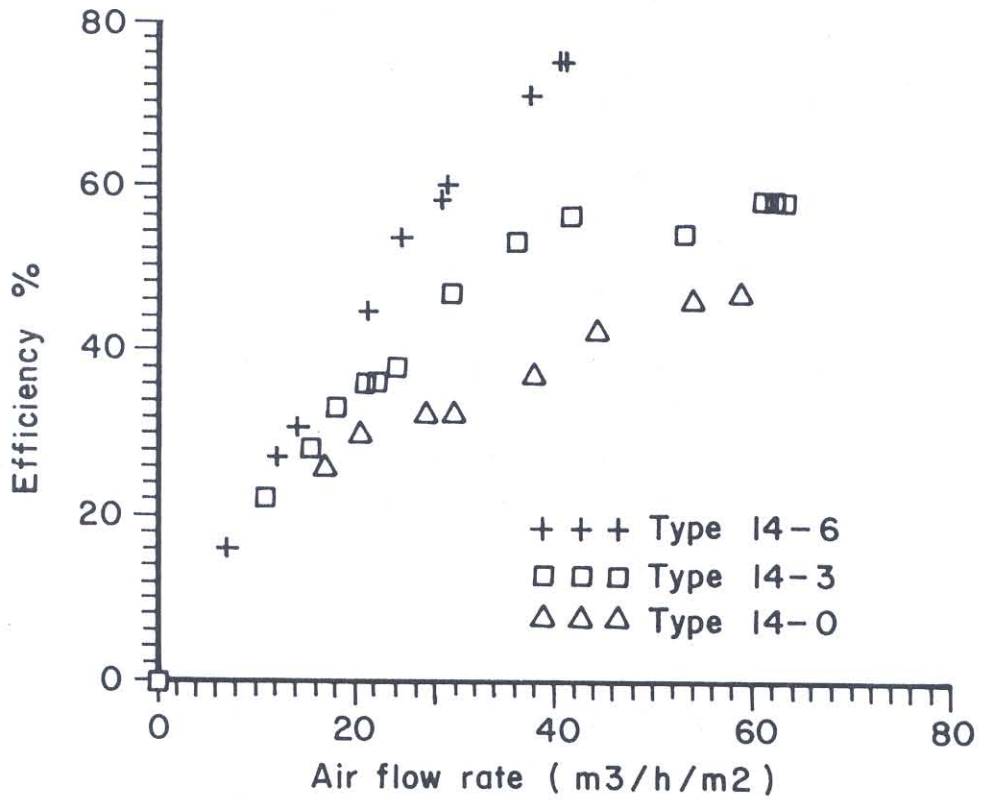


Fig. 8. Efficiency versus air flow rate.

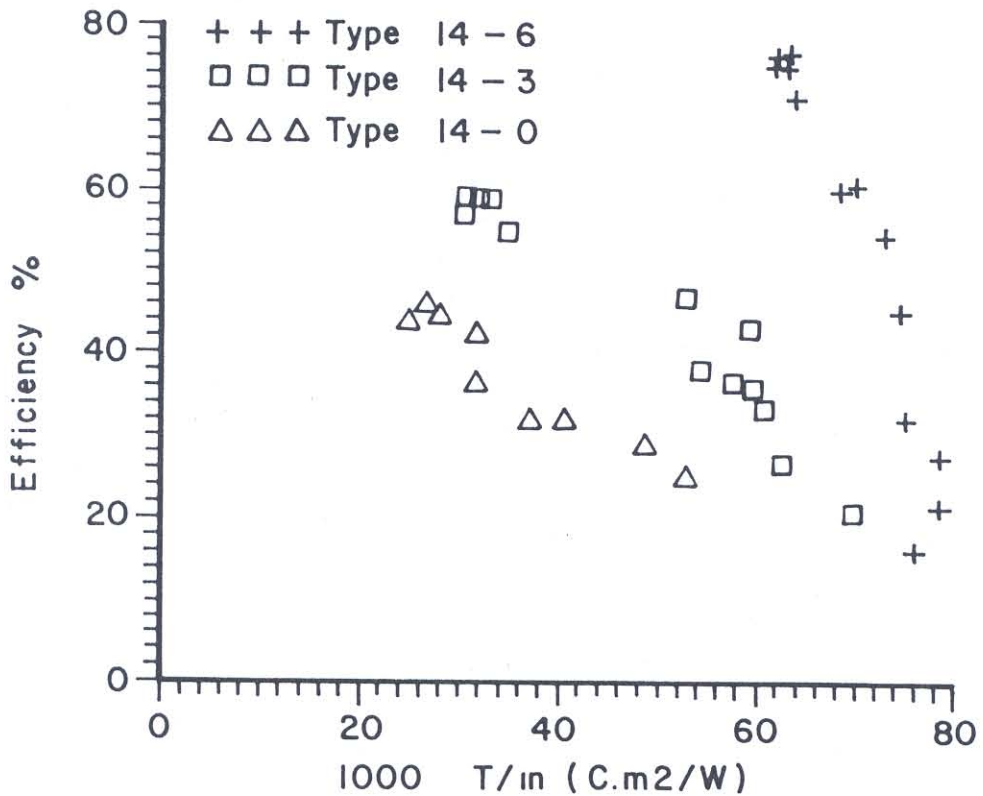
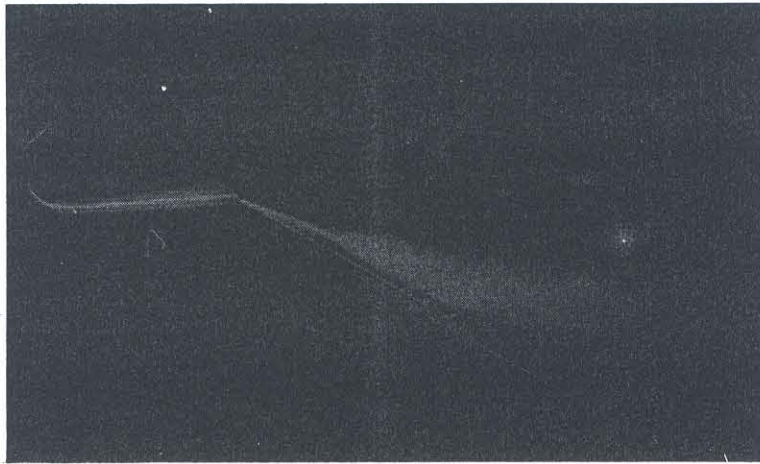


Fig. 9. Efficiency as function of  $\Delta T/I_N$ .

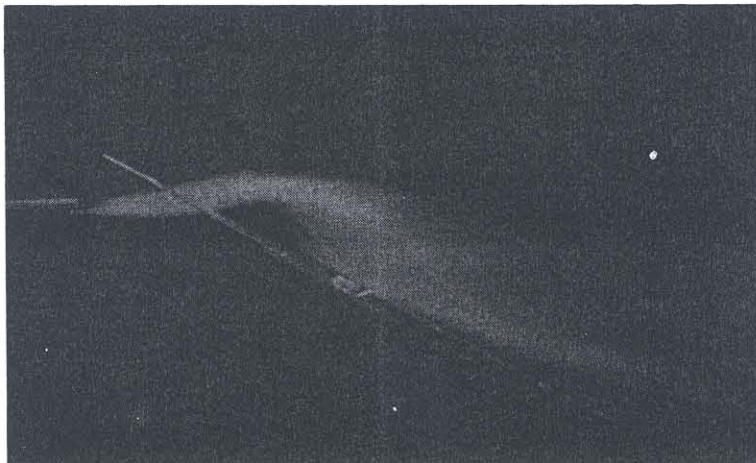




a)  $\beta = 50^\circ$   $i = 10^\circ$



b)  $\beta = 50^\circ$   $i = 30^\circ$



c) The depression created above the wing inhale the neighborhood air.

Fig. 10. Depression at the extrados of a delta wing.



forming the select series of angles: ...18.4°, 19.5°, 20.7°, 22.2°, 24.2°, 26.6°, 30°, 35.3°, 45°, 54.7°, 63.4°, 68.6°, 72°, 74.5°, 76.6°, 77.8°...

It would be interesting to observe the turbulence caused by the delta wings on the insulation with large "i" incidence and moderate  $\phi$  (Fig 18-b). Conversely, with low incidence and apex angle, the whirls "stick" to the wings ( $\gamma$  weak). It would also be interesting to place the wings on or under the absorber. Under the absorber, the delta wings will have besides the aeraulic effect, a thermal effect like the winglets. The results of the measurement of efficiency with the wings on the insulation are represented by the curves of Fig. 12.

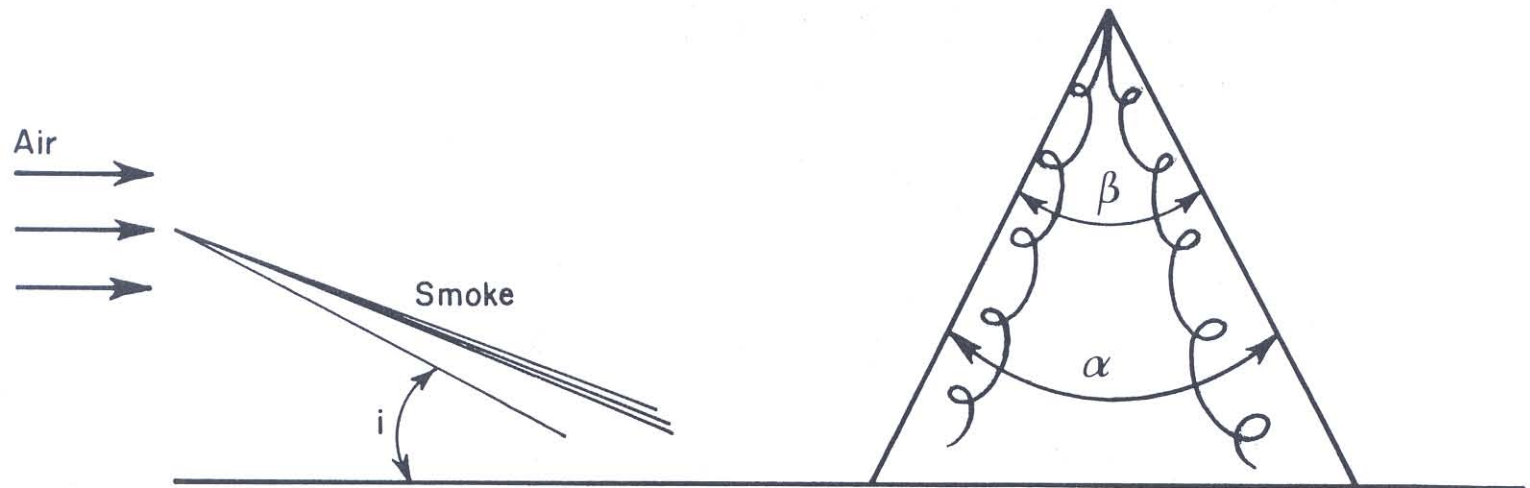


Fig. 11. Formation of whirls at the extrados of a delta wing.

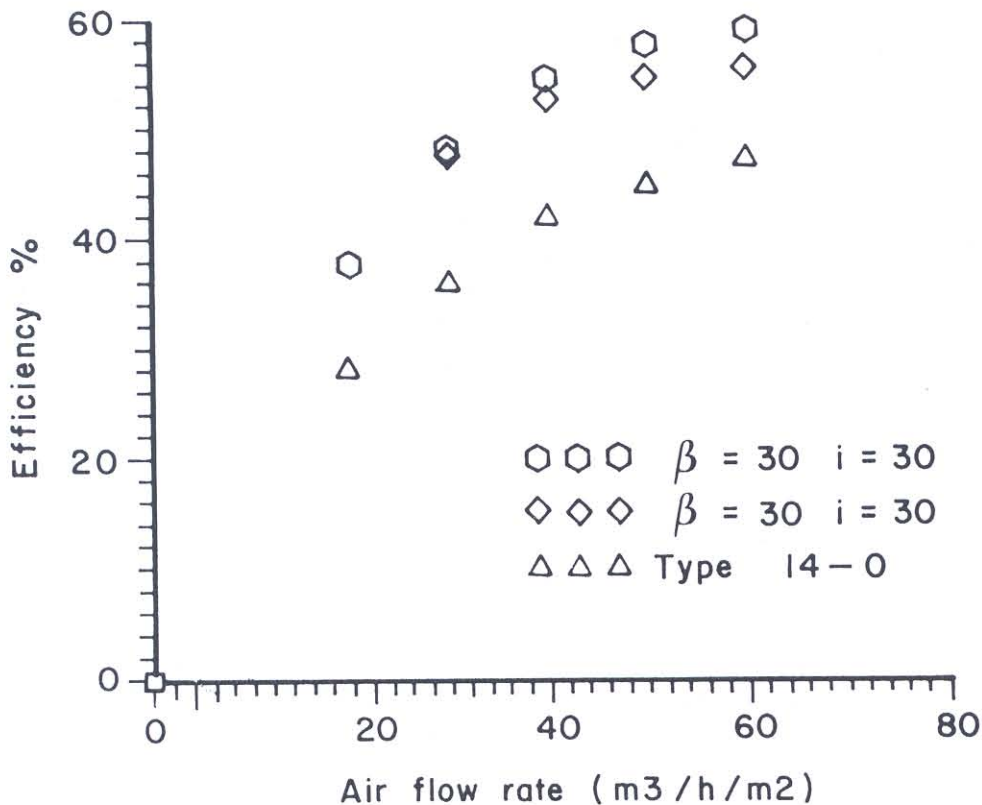


Fig. 12. Efficiency versus air flow rate (delta wing-shaped baffles).

## 6. CONCLUSION

The different air flows formed in the collector with various baffle types have been determined visually. The dead zones as well as the formation of whirls created in the baffles were identified. The visualization is a pragmatic way to make the first choice (14-6). The chosen baffles create only a low pressure drop increase compared to small baffles (some mm of water).

The efficiency measurements confirmed these results and proved that an 80 % efficiency could be reached for a flow of  $45 \text{ m}^3/\text{m}^2\text{h}$ . The  $\Delta T$  reaches  $55^\circ\text{C}$  for a flux of  $1000 \text{ W}/\text{m}^2$ . The performances are hence better than those of type 1-c and 1-d in the literature review.

The use of wing-shaped baffles located on or under the absorber is a promising way. Besides the aeraulic effect, these baffles showed a thermal effect (winglets), thus increasing the heat exchange area, like fins, and hence the efficiency.

## APPENDIX

$$U_1 = h_{pva} + h_{cpa} - \frac{h_{pv}^2}{h_{pv} + h_{vc}}$$

$$U_2 = \frac{h_{pv} h_{vc}}{h_{pv} + h_{vc}} + \frac{h_{cpa}}{2} + \frac{h_{cba}}{2} + U_b$$

$$U_3 = h_{cba} + U_b$$

$$U_4 = (h_{cba} + h_{cpa})/2$$

$$U_5 = h_{cpa}/U_1$$

$$U_6 = m.ca + U_4 - U_4 U_5$$

$$U_7 = m.ca - U_4 + U_2 U_5$$

$$U_8 = h_{cba} - U_3 U_5$$

$$U_9 = h_{rpb}/U_1$$

$$U_{10} = U_2 U_9 + U_b + h_{cba}/2$$

$$U_{11} = U_3 U_9 + U_b + h_{cba} + h_{rpb}$$

$$U_{12} = U_4 U_9 + h_{cba}/2$$

## 7. REFERENCES

1. Sfeir, 1981. Ingénierie des systèmes solaires. *Technique et documentation*: 115-116.
2. Chauliaguet. 1981. *L'énergie Solaire Dans le Bâtiment*. Paris: Eyrolles.
3. Barrabe. 1980. *Energies Nouvelles. Energies Pour la Vie*. Aix en Prov: Edisud.
4. Bargava-Garg-Sharma. 1982. Evaluation of the Performance of Air Heaters of Conventional Designs. *Solar Energy* 29( 6): 523-533.
5. Wijesundera, N.E. 1982. Thermal performance study of two pass solar air heaters. *Solar Energy* 28( 5): 363-370.
6. Biondi, P.; Cicala, L.; and Farina, G. 1988. Performance analysis of solar air heaters of conventional design. *Solar Energy* 41(8):101-107.
7. Choudhury -Garg. 1991. Evaluation of jet plate solar air heater. *Solar Energy* 46(4):119-209.
8. Benslama-Boughaleb-Ouard-Leray. 1986. Etudes de capteurs solaires à air. *Journées de l'A.U.M.* Université de Valenciennes.
9. Benslama, R. 1987. Contribution à l'étude et au développement de pompes et capteurs solaires. Thèse de spécialité en énergétique. Université de Valenciennes-France.
10. Ouard, S. 1989. Optimisation des formes et dispositions d'obstacles dans la veine d'air mobile des capteurs solaires à air à deux couches d'air en vue de la maximisation du couple rendement-élévation de température. Thèse de spécialité en énergétique. Université de Valenciennes.
11. Benslama R.; Bouabdallah, M.; and Le Ray, M. 1994. Amélioration de la turbulence dans les capteurs solaires à air par l'usage de chicane en vue d'accroître le rendement. 1ère. *Conférence Maghrébine du Génie des Procédés- Marrakech*: 727-730.
12. Benslama R.; Bouabdallah, M. ; and Le Ray, M. 1995. Introduction de chicanes dans les capteurs solaires à air en vue de favoriser la turbulence qui accroît le couple rendement-élévation de température. In *The Second International Thermal Energy Congress*. Agadir:109-114.
13. Le Ray, M. 1980. Dialogue du physicien et de l'esthète. *Communication et langage No 45*, Paris.
14. Le Ray, M.; Deroyon; and Minair, C. 1985. Critères angulaires de stabilité d'un tourbillon hélicoïdal ou d'un couple de tourbillons rectilignes, rôle des angles privilégiés dans l'optimisation des ailes, voiles, coques des avions et navires, *Revue de l'association Technique Maritime et Aéronautique*.
15. Minair, C. 1987. Les angles privilégiés, grands invariants universaux: une approche par la dynamique des fluides, l'esthétique, et la physio-biologie. Thèse de Doctorat d'Etat. Université de Valenciennes.